

## **A PROXIMITY-FED ANNULAR SLOT ANTENNA WITH DIFFERENT A BAND-NOTCH MANIPULATIONS FOR ULTRA-WIDE BAND APPLICATIONS**

**E. E. M. Khaled<sup>1,\*</sup>, A. A. R. Saad<sup>2</sup>, and D. A. Salem<sup>3</sup>**

<sup>1</sup>Elec. Eng. Dept., Assiut University, Assiut, Egypt

<sup>2</sup>Elec. Eng. Dept., Minia University, Minia, Egypt

<sup>3</sup>Microstrip Dept., Electronics Research Institute, Giza, Egypt

**Abstract**—A proximity-fed annular slot antenna for UWB applications with a band rejection using different techniques is presented. The proposed antenna provides an UWB performance in the frequency range of  $\approx 2.84$  to  $\approx 8.2$  GHz with relatively stable radiation parameters. Three different techniques to construct a resonant circuit for the proposed antenna are investigated to achieve the band-notch property in the band  $\approx 5.11$  to  $\approx 5.69$  GHz band which include the WLAN and HIPERLAN/2 services without degrading the UWB performance of the antenna. Three resonators are considered; a single complementary split ring resonator (CSRR), a complementary spiral loop resonator (CSLR) and a spurline slot. Furthermore, the band-notched resonance frequency and the bandwidth can be easily controlled by adjusting the dimensions of the resonator. The proposed antenna is simulated, fabricated and measured. The measured data show very good agreements with the simulated results. The proposed antenna provides almost omnidirectional patterns, relatively flat gain and high radiation efficiency over the entire UWB frequency excluding the rejected band.

### **1. INTRODUCTION**

Since the Federal Communications Commission (FCC) in USA released the commercial use of the ultra-wide band (UWB) radio system (3.1–10.6 GHz) in 2002, various types of planar UWB antennas have been proposed and developed for use in the wireless communication

---

*Received 31 October 2011, Accepted 22 December 2011, Scheduled 28 December 2011*

\* Corresponding author: Elsayed Esam M. Khaled (esamk54.2000@hotmail.com).

systems [1–3]. The existing upper WLAN band (5.15–5.35 GHz, 5.725–5.825 GHz) in USA and HIPERLAN/2 band (5.15–5.35 GHz, 5.47–5.725 GHz) in Europe may overlap with the new UWB services and applications [4]. Therefore to avoid such overlapping UWB antennas with band-notch property are desirable. The band-notch can be achieved via the antenna design instead of adding new circuits, such as filters, to the communication systems. Many techniques have been proposed and developed to obtain the band-notch property through the antenna design such as; etching different kinds of slots on the patch or on the ground plane [5–7], or adding parasitic elements using folded strips to the antenna [8], or inserting a spurline by etching one slot on a microstrip line of the antenna [9–11]. Recently, the unwanted frequency bands are notched using resonators such as a split ring resonator (SRR), or its negative image which is a complementary split ring resonator (CSRR) [12–14] as well as the spiral loop resonator (SLR) [15]. Because of these structures are electronically small resonator with a very high  $Q$  it can be considered as filters providing a sharp notch or pass of a certain frequency band. These resonators structures have resonance behavior when excited with suitable electromagnetic fields. Moreover it shows unusual properties such as negative permeability and permittivity near the resonance frequency region [16].

Most of the research of the UWB antennas in the literature focused on designing planar UWB band-notched antennas with microstrip feed-line technique or CPW-feed technique. In this work, a different feeding technique, the proximity-feed in which a microstrip line placed in the one side of the substrate of the antenna facing the patch that placed in the other side of the substrate, is adopted. The patch of the proposed antenna that yields an UWB response is a circular patch placed non-concentrically inside a ground plane aperture (GPA). The band-notch property is obtained by using either one of the following three different techniques. The first technique uses a single complementary split ring resonator (CSRR) etched off the circular patch. The second technique uses a complementary spiral loop resonator (CSLR) etched off the circular patch, whereas the third technique uses a spurline etched off the microstrip line. The main idea of these techniques is to adjust the resonant frequency of the etched slots with the required rejected band, to provide the band-notch property over the desired frequency range. The resonant frequencies can be achieved by adjusting the dimensions of the slots. The proposed band-notched antenna is smaller in size (by almost 35% smaller than the other similar antennas) and less in complexity compared to other planar transmission lines (either CPW or microstrip) introduced in the literature [17]. Besides, the proposed

antenna has a better performance regarding the gain and radiation efficiency over the operated frequency band. The design details along with simulation results and experimental data are presented and discussed in Section 2. The conclusion of this work is outlined in Section 3.

## 2. DESIGN METHODOLOGY

This section describes the antenna geometry and the design process. A full wave analysis of the proposed structures is obtained by using the electromagnetic software, Zeland IE3D which is based on Method of Moments (MoM) numerical technique. The design goals are to achieve

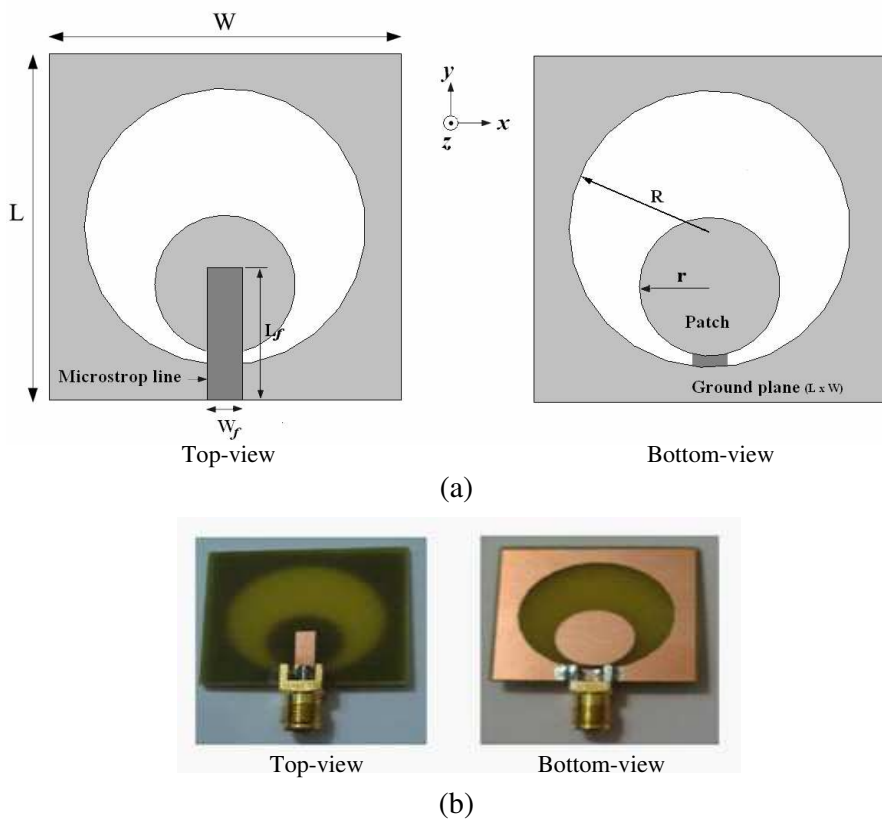


**Figure 1.** (a) Geometry of the proposed UWB antenna. (b) Photographs of the fabricated antenna.

impedance bandwidth cover the UWB frequency spectrum with good gain, stable radiation patterns across the whole desired band excluding the rejected band (the band-notch) that obtained by three different techniques. Analysis of several parametric studies to optimize the UWB antenna design ending up with the best possible impedance bandwidth with appropriate band-notch function is investigated.

## 2.1. Design of UWB Prototype Antenna

The geometry of the proposed prototype antenna is illustrated in Figure 1(a). The antenna is fabricated on a  $30 (L) \times 30 (W) \text{ mm}^2$  FR4 substrate with the relative permittivity of 4.7, a loss tangent  $\tan \delta = 0.02$  and a thickness  $h = 1.5 \text{ mm}$ . A circular radiating patch of radius  $r = 6.0 \text{ mm}$  is placed non-concentrically inside a circular slot of radius  $R = 12.0 \text{ mm}$  etched off the ground plane. The circular slot represents a ground plane aperture (GPA). The patch and the GPA are centered vertically with the ground plane. The distance between the lower edge of the circular patch and the lower edge of the circular slot is  $1.0 \text{ mm}$ . The circular patch is excited through a  $50 \Omega$  proximity-feed microstrip line placed on the other side of the substrate, with width  $w_f = 3.0 \text{ mm}$  and length,  $l_f = 11.5 \text{ mm}$  [18]. Photographs of the top and bottom views of the fabricated prototype antenna are shown in Figure 1(b).

The simulated results of the return loss of the antenna with different values of  $R$ , and  $r$  and keeping the other dimensions the same, as stated earlier, are shown in Figures 2 and 3 respectively.

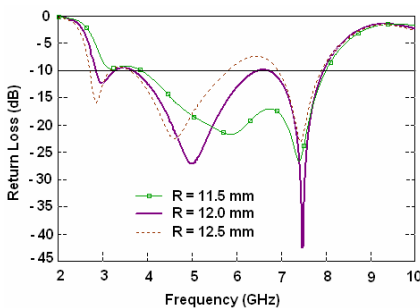


**Figure 2.** Simulated return loss versus frequency of the proposed antenna for different values of the radius  $R$  with  $r = 6.0 \text{ mm}$ ,  $w_f = 3.0 \text{ mm}$ ,  $l_f = 11.5 \text{ mm}$ .

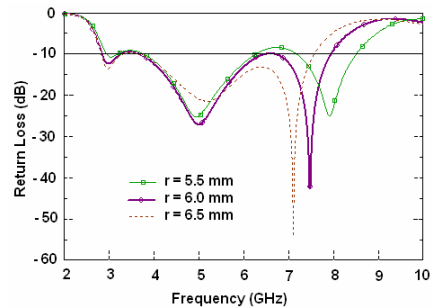


**Figure 3.** Simulated return loss versus frequency of the proposed antenna for different values of the radius  $r$  with  $R = 12.0 \text{ mm}$ ,  $w_f = 3.0 \text{ mm}$ ,  $l_f = 11.5 \text{ mm}$ .

The results show that, for  $R = 12.0$  mm and  $r = 6.0$  mm the 10 dB return loss has the highest impedance bandwidth. Simulation results of the return loss with different values of  $l_f$  and  $w_f$  of the microstrip feed-line are shown in Figure 4 for  $r = 6.0$  mm, and  $R = 12.0$  mm. The optimal parameters are  $l_f = 11.5$  mm, and  $w_f = 3.0$  mm for a better impedance bandwidth. It is apparent that the prototype antenna has impedance bandwidth from 2.85 GHz to 7.95 GHz which is suitable for UWB indoor communications.

The fabricated prototype antenna was tested using vector network

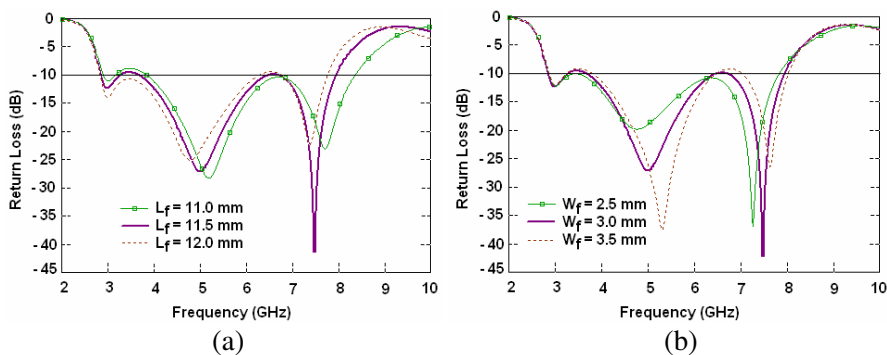


**Figure 4.** Simulated return loss versus frequency of the proposed antenna for different values of the length,  $l_f$  and with  $w_f$  of microstrip line with  $r = 6.0$  mm, and  $R = 12.0$  mm, (a) the results are for  $w_f = 3.0$  mm and different values of  $l_f$ , (b) the results are for  $l_f = 11.5$  mm and different values of  $w_f$ .

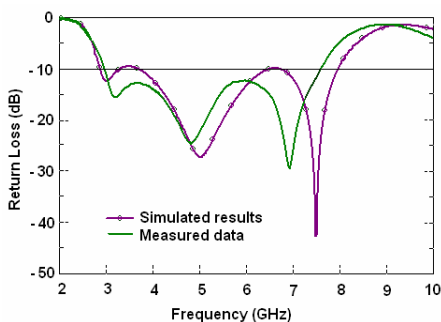


**Figure 5.** Measured data and simulated results of the return loss versus frequency of the antenna with  $r = 6.0$  mm,  $R = 12.0$  mm,  $w_f = 3.0$  mm, and  $l_f = 11.5$  mm.

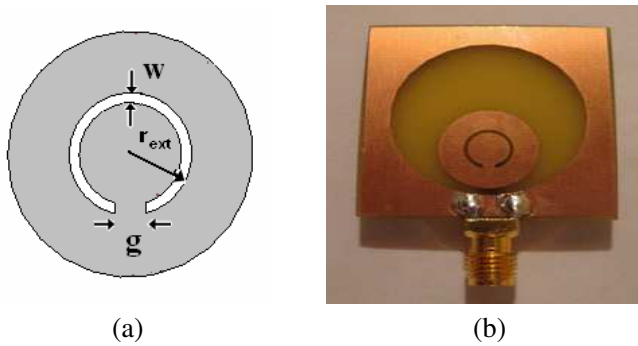


**Figure 6.** (a) Configuration of a single CSRR etched off the circular patch. (b) Photograph of the bottom-view of the proposed band-notched antenna using a Single CSRR.

analyzer (Agilent HP8719). Figure 5 illustrates the measured data and the simulated results of the return loss as a function of frequency. The simulation results show an impedance bandwidth from 2.85 GHz to 7.95 GHz whereas the measured data show a less bandwidth, in spite of the resemblance of the two curves. This minor discrepancy may be attributed to the fabrication tolerance, and to the spatial closeness of the connector to the radiating slot and the patch.

## 2.2. A Band-notch Manipulations

Band-notched property is obtained by modifying the UWB prototype antenna using three different techniques based on etching off the radiating patch or the feeding microstrip line with resonating slots. In order to utilizing these resonating slots the  $S$ -parameters of a basic resonator cell on  $50\ \Omega$  microstrip line are simulated using the electromagnetic simulation. Such simulation allows deciding the size of the resonator by observing the stop band frequency [19–22]. The dimension and location of the resonating slot control the band rejection and the bandwidth of the antenna.

The first band rejection technique is based on etching off the circular patch by a single complementary split ring resonator (CSRR) centered with the patch as shown in Figure 6. A model of a single CSRR underneath a microstrip line and the resultant  $S$ -parameter are shown in Figure 7. The substrate of FR4 with a relative dielectric constant of 4.7 and thickness of 1.5 mm is used for simulation. The dimensions of the CSRR element are: The external radius is  $r_{ext} = 3.0$  mm, the gap is  $g = 1.5$  mm, and the uniform width of the ring is

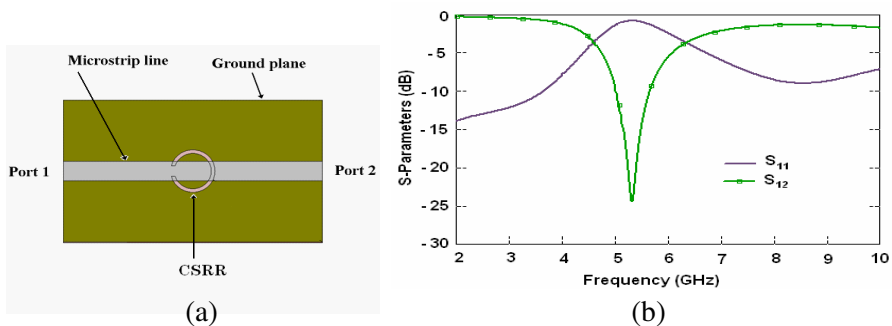


**Figure 7.** (a) A basic cell of a single CSRR underneath a microstrip line. (b) Simulated results of the  $S$ -parameters.

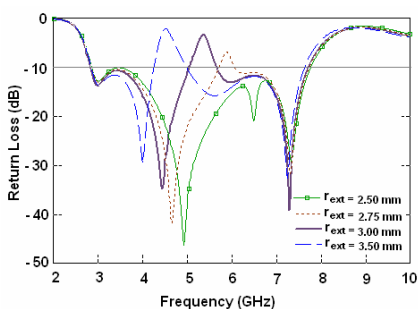


**Figure 8.** Simulated return loss versus frequency of the prototype antenna integrated with a single CSRR with  $w = 0.5$  mm,  $g = 1.5$  mm,  $r = 6.0$  mm,  $R = 12.0$  mm,  $w_f = 3.0$  mm, and  $l_f = 11.5$  mm, for different values of  $r_{ext}$ .

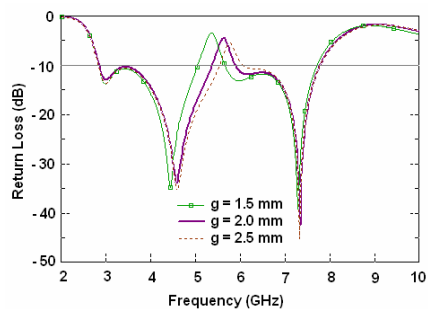


**Figure 9.** Simulated return loss versus frequency of the prototype antenna integrated with a single CSRR with  $r_{ext} = 3.0$  mm,  $w = 0.5$  mm,  $r = 6.0$  mm,  $R = 12.0$  mm,  $w_f = 3.0$  mm, and  $l_f = 11.5$  mm, for different values of  $g$ .

$w = 0.5$  mm. These physical parameters of the simulated resonator on the microstrip line have an attenuation pole around 5.36 GHz, with attenuation level (-25 dB) of the stop band.

Dimensions adjustment of the slot resonator can give the proposed antenna appropriate UWB performance and band-notching suitable to avoid interference with WLAN and HIBERLAN/2 services. Figures 8 and 9 show the effect of the dimensions of a single complementary split ring resonator etched off the patch and concentric with it to control the band-notching and bandwidth characteristics of the antenna. It

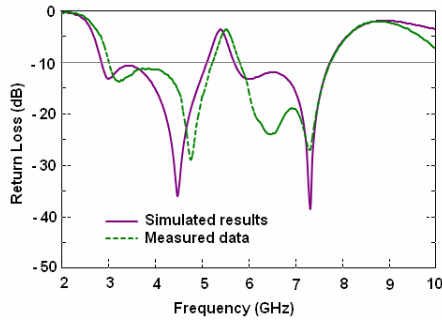


**Figure 10.** Measured data and simulated results for the return loss versus frequency of the prototype antenna integrated with a single CSRR with  $r_{ext} = 3.0$  mm,  $g = 1.5$  mm,  $w = 0.5$  mm,  $r = 6.0$  mm,  $R = 12.0$  mm,  $w_f = 3.0$  mm, and  $l_f = 11.5$  mm.

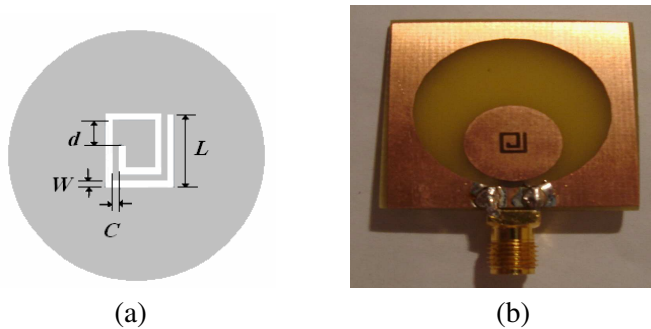


**Figure 11.** (a) Configuration of the CSLR etched off the circular patch. (b) Photograph of the bottom-view of the proposed band-notched antenna using a CSLR.

is observed that the antenna with CSRR of  $r_{ext} = 3.0$  mm and  $g = 1.5$  mm and all other parameters kept constant as;  $w = 0.5$  mm,  $R = 12.0$  mm,  $r = 6.0$  mm,  $w_f = 3.0$  mm, and  $l_f = 11.5$  mm, can be utilized over the bandwidth 2.83–7.72 GHz with notched frequency band from 5.06–5.65 GHz. The measured data and simulated results of the return loss of the prototype antenna integrated with a single CSRR are illustrated in Figure 10. Good agreement between the measured data and the simulated results is obtained.

The second band rejection technique is based on etching off the circular patch by a complementary spiral loop resonator (CSLR) concentric with the patch as shown in Figure 11. A model of a CSLR

underneath a microstrip line and the resultant  $S$ -parameter are shown in Figure 12. The substrate is from FR4 material with a relative dielectric constant of 4.7 and thickness of 1.5 mm. The dimensions of the CSLR element are:  $L = 3.2$  mm,  $w = 0.4$  mm,  $c = 0.4$  mm and  $d = 1.2$  mm. These physical parameters of the simulated resonator have an attenuation pole around 5.38 GHz of the stop band with attenuation level around  $-15$  dB.

Figure 13 shows the effect of the variation of  $L$ , on the return loss. The results show that as  $L$  decreases the center frequency

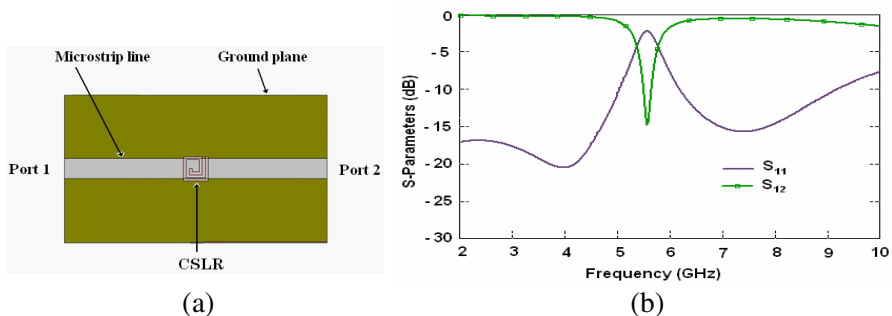


**Figure 12.** (a) A basic cell of a CSLR underneath a microstrip line. (b) Simulated results of the  $S$ -parameter.

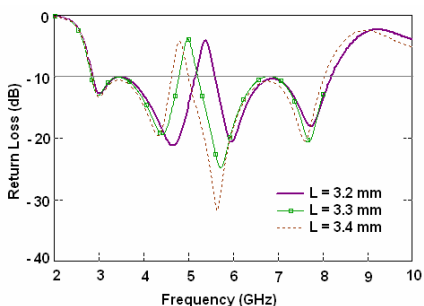


**Figure 13.** Simulated return loss versus frequency of the proposed antenna integrated with CSLR for different values of the spiral loop length,  $L$ , with  $w = c = 0.4$  mm,  $d = 1.2$  mm,  $r = 6.0$  mm,  $R = 12.0$  mm,  $w_f = 3.0$  mm, and  $l_f = 11.5$  mm.

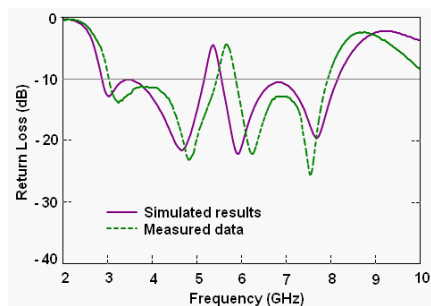


**Figure 14.** Measured and simulated return loss versus frequency of the proposed antenna integrated with a single CSLR with  $L = 3.2$  mm,  $w = c = 0.4$  mm,  $d = 1.2$  mm,  $r = 6.0$  mm,  $R = 12.0$  mm,  $w_f = 3.0$  mm, and  $l_f = 11.5$  mm.

of the band notch increases. By adjusting the dimensions to be  $L = 3.2\text{ mm}$ ,  $w = 0.4\text{ mm}$ ,  $c = 0.4\text{ mm}$ , and  $d = 1.2\text{ mm}$  a band rejection from 5.16 GHz to 5.59 GHz is obtained. The measured data and the simulated results of the return loss of the prototype antenna integrated with a CSLR are illustrated in Figure 14. Good agreement between the measured data and the simulated results is obtained.

The third alternative technique to achieve a well defined rejection band uses a spurline integrated on the microstrip line, as shown in Figure 15. A spurline is a simple microstrip defected structure (MDS), which is realized by etching one slot on a microstrip line. The good feature of a spurline filter is that its physical structure is completely

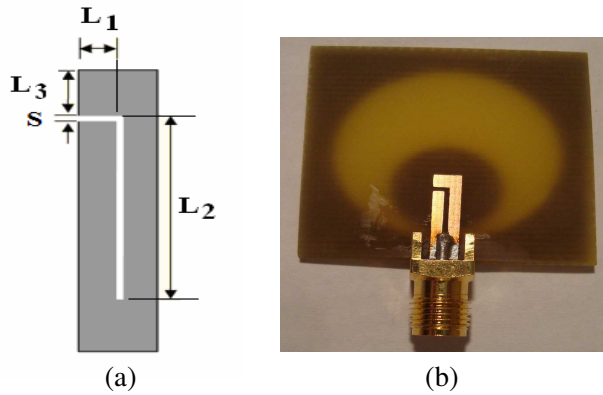


**Figure 15.** (a) Configuration of a spurline integrated on the microstrip line. (b) Photograph of the top-view of the proposed band-notched antenna using a spurline.

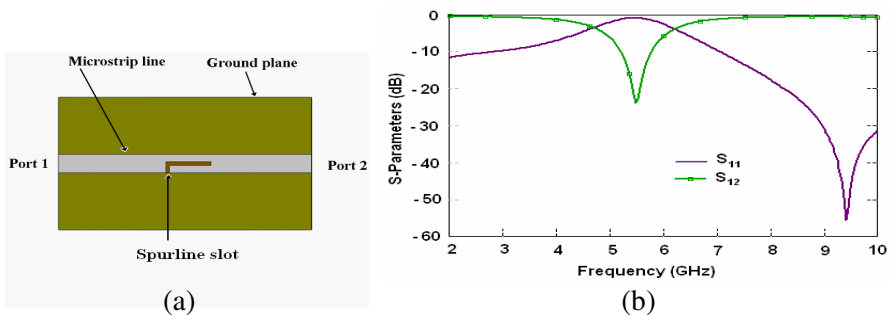


**Figure 16.** (a) A model of a basic cell of the microstrip line integrated with a spurline. (b) Simulated results of the  $S$ -parameter.

contained within the boundaries of the microstrip line. The spurline has three parameters used to optimize the band-notch performance which are the length  $L_2$ , the height  $L_1$ , and the width  $S$  of the slot. The slot length of the spurline,  $L_2$  is approximately a quarter of the wavelength at the desired stop frequency band, measured in the microstrip line material.

A parametric study for the spurline is demonstrated here using a model of a spurline underneath a microstrip line. Figure 16 shows the model and the resultant  $S$ -parameters obtained using the IE3D simulator. The dimensions of the spurline are:  $L_2 = 8.0$  mm,  $L_1 = 0.9$  mm and  $S = 0.5$  mm. The substrate of FR4 with a relative dielectric constant of 4.7 and thickness of 1.5 mm is used for the simulation. The spurline is etched on a  $50\ \Omega$  microstrip line which have 2.73 mm width. The simulation results shown in Figure 16(b) demonstrate that these physical dimensions have an attenuation pole around 5.48 GHz, with attenuation level ( $-24$  dB) at the center frequency of the stop band. Also the results show that integrating a spurline etched in the microstrip line, considerably improves  $S_{11}$  to almost  $-55.5$  dB in the passband around the frequency 9.4 GHz, which improve the antenna bandwidth with the required band-notch.

The spurline shown in Figure 15(a) consists of three lengths  $L_1$ ,

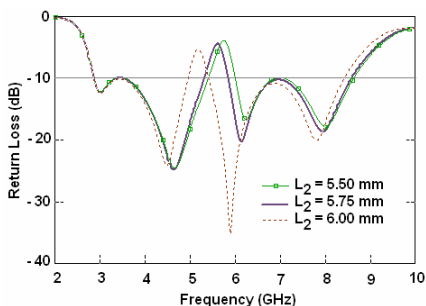


**Figure 17.** Simulated return loss versus frequency of the proposed antenna integrated with spurline with different slot lengths  $L_2$ . The other dimensions are  $L_1 = 1.75$  mm,  $L_3 = 1.25$  mm,  $S = 0.5$  mm,  $w_f = 3.0$  mm,  $l_f = 11.5$  mm,  $r = 6.0$  mm, and  $R = 12.0$  mm.

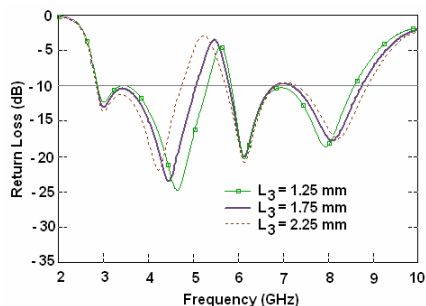


**Figure 18.** Simulated return loss versus frequency of the proposed antenna integrated with spurline with different slot locations  $L_3$  and with  $L_1 = 1.75$  mm,  $L_2 = 5.75$  mm,  $S = 0.5$  mm,  $w_f = 3.0$  mm,  $l_f = 11.5$  mm,  $r = 6.0$  mm, and  $R = 12.0$  mm.

$L_2$ , and  $L_3$ . These lengths were optimized to obtain the band-notch performance of the proposed antenna. Results of the parametric study of the simulated return loss of the proposed antenna using this

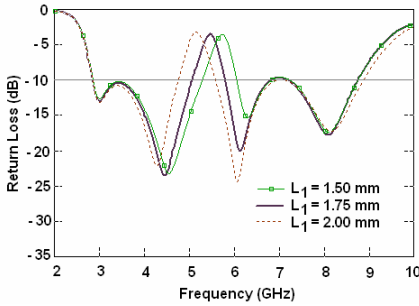


**Figure 19.** Simulated return loss versus frequency of the proposed antenna integrated with spurline with different slot length  $L_1$  and with  $L_2 = 5.75$  mm,  $L_3 = 1.75$  mm,  $S = 0.5$  mm,  $w_f = 3.0$  mm,  $l_f = 11.5$  mm,  $r = 6.0$  mm, and  $R = 12.0$  mm.

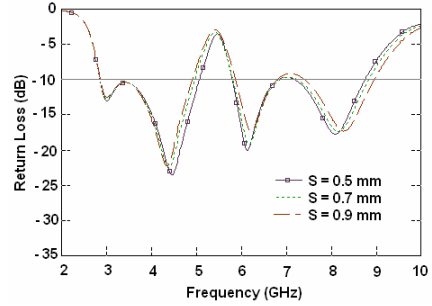


**Figure 20.** Simulated return loss versus frequency of the proposed antenna integrated with spurline with different slot width  $S$  and with  $L_1 = L_3 = 1.75$  mm,  $L_2 = 5.75$  mm,  $w_f = 3.0$  mm,  $l_f = 11.5$  mm,  $r = 6.0$  mm, and  $R = 12.0$  mm.

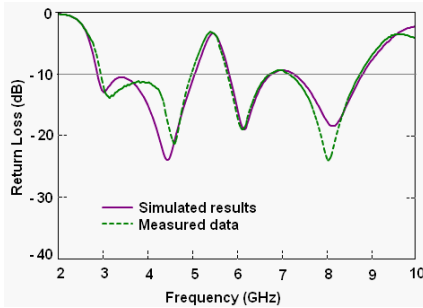


**Figure 21.** Measured data and simulated results of the return loss versus frequency of the prototype antenna integrated with a spurline with  $L_1 = L_3 = 1.75$  mm,  $L_2 = 5.75$  mm,  $S = 0.5$  mm,  $w_f = 3.0$  mm,  $l_f = 11.5$  mm,  $r = 6.0$  mm, and  $R = 12.0$  mm.

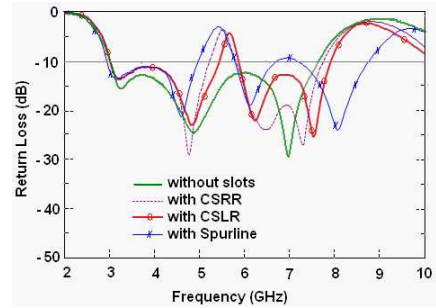


**Figure 22.** Measured data of the return loss versus frequency of the prototype antenna integrated with either one of the three different resonating slots.

technique are shown in Figures 17–20. The optimal dimensions of the spurline to obtain a band rejection at 5.5 GHz are,  $L_1 = L_3 = 1.75$  mm,  $L_2 = 5.75$  mm with a uniform width  $S = 0.5$  mm. This optimal design provides a bandwidth from 2.85 to 8.75 GHz with a sharp band rejection from 5.07 to 5.79 GHz. Hence a narrow frequency band can be filtered out while maintaining good matching over the rest of the UWB frequency band. It is observed that, the spurline enhance impedance bandwidth of the prototype antenna by almost 800 MHz due to spurline characteristics. The measured data and the simulated results of the return loss (RL) of the prototype antenna integrated with a spurline are illustrated in Figure 21. Good agreement between the measured data and the simulated results is obtained.

The effect of the different resonating slots with its corresponding optimal dimensions used in the three techniques as stated earlier on the return loss of the prototype antenna is presented in Figure 22 for comparison. Good impedance matching was observed throughout the whole operation band. The prototype antenna with spurline has a wider impedance bandwidth with a suitable band rejection of a central frequency at 5.5 GHz. The frequency response of the band-notched can be easily tuned by adjusting the dimensions of the slots, which control

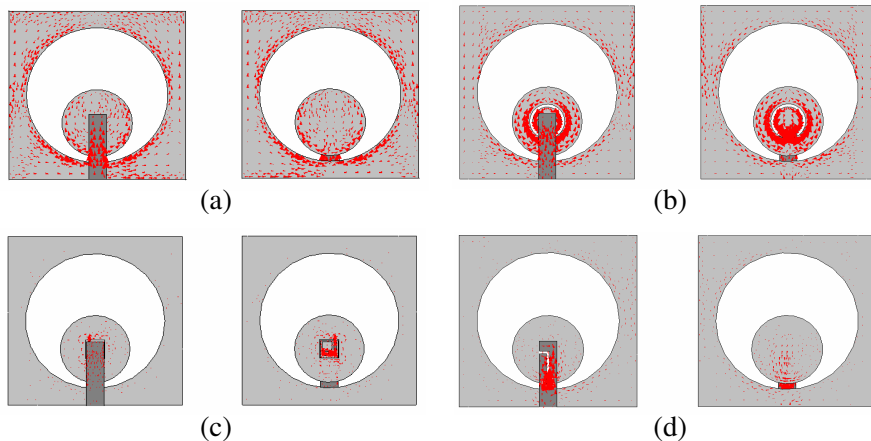


**Figure 23.** Simulated surface current distributions of the proposed antenna with and without the resonating slots at the top and bottom view of the antenna at the center frequency of the band-notch, (a) the antenna operated at 5.5 GHz without a resonating slots, (b) the antenna integrated with CSRR operated at 5.36 GHz, (c) the antenna integrated with CSLR operated at 5.38 GHz, (d) the antenna integrated with spurline operated at 5.46 GHz.

the corresponding resonance frequency.

The simulated current distributions of the proposed antenna at the center frequency of the band-notch are shown in Figure 23. The current distributions for the antenna without the band-notched resonating slots are nearly uniform on the antenna surface and around the ground plane aperture. For the antenna integrated with the CSRR element the currents are concentrated around the element and distributed uniformly on the ground plane due to the coupling with the slot. In case of the antenna integrated with CSLR slot the currents are concentrated around the slot with small currents on the ground conductor. The

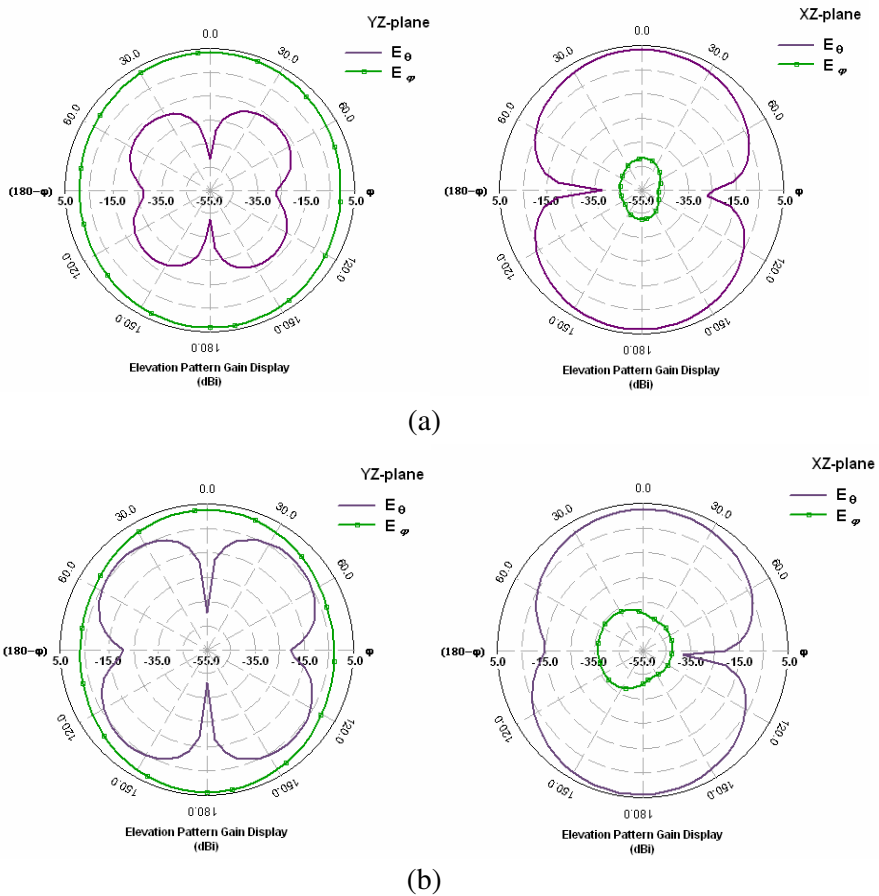


**Figure 24.** Simulated radiation patterns of  $E_\theta$  and  $E_\phi$  in the  $yz$  and  $xz$  planes for the UWB prototype antenna, (a) at 4 GHz, (b) at 6 GHz.

CSLR slot acts as an inductor which couples energy from an incident time-varying magnetic field to it to produce a loop current in the spiral. The interaction between the spiral inductance and spiral capacitance provides the resonant behavior of the slot [15]. For the prototype antenna integrated with spurline slot the currents are mainly exists around the bottom of the slot and the ground plane. The slot gap on the spurline provides a capacitive effect while the narrow line exhibits an inductive effect. Thus, the effective permittivity of the dielectric substrate increases which improves the resonance behavior of the slot on the spurline.

The radiation characteristics of the prototype antenna are also investigated. Figure 24 illustrate the simulated far-field radiation patterns of  $E_\theta$  and  $E_\varphi$  in the  $yz$  and  $xz$  planes at two suggested frequencies 4.0 GHz and 6.0 GHz in the pass band of the antenna. The figure demonstrates that the prototype antenna is characterized by omnidirectional patterns in the  $yz$  plane ( $E$ -plane), while it is a quasi-omnidirectional pattern in the  $xz$  plane ( $H$ -plane). Some other simulated results (not shown here) show that the radiation patterns of the proposed antenna with any of the three different resonating slots are almost the same as those of the prototype antenna, whereas a little deviation is observed in the cross polarization in the  $xz$ -plane. The highest cross-polarized level is appeared when the prototype antenna integrated with spurline.

Figure 25 illustrates the simulated peak gain and radiation efficiency versus frequency for the proposed antenna with and without the band-notched resonating slots. The illustrated results reveal that

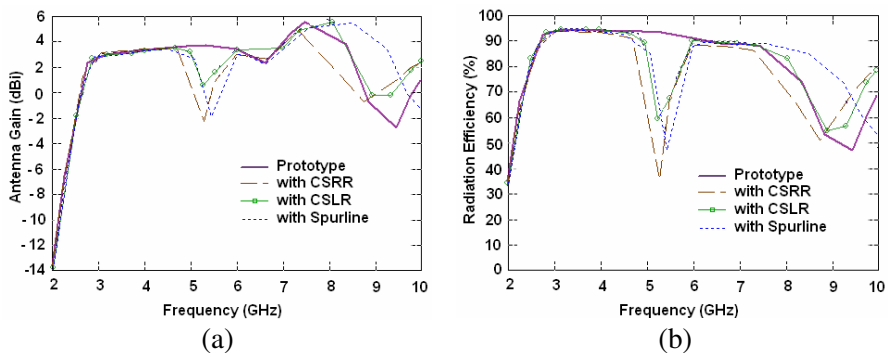


**Figure 25.** (a) Simulated peak gain, and (b) radiation efficiency, versus frequencies of the proposed antenna with and without the resonating slots.

the gain for the antenna with or without the slots varies from 3.05 dBi to 5.86 dBi over the pass band frequency range. Implementing any of the slots reduces the gain of the antenna sharply to about  $-2.9$  dBi, at the designed notched frequency. The radiation efficiency is almost 90% excluding the rejected band.

### 3. CONCLUSION

A proposed ultra-wideband annular slot antenna with frequency band-notch property is presented. Matching between a circular radiator patch and the 50 Ohm microstrip line is manipulated through a proximity-feed technique. Incorporating either a complementary split ring resonator (CSR) or a complementary split loop resonator (CSLR) or a spurline to the antenna provides band-notch characteristics. The effects of adding such resonating slots on the performance of the antenna are demonstrated. The designed antenna satisfies a 10 dB return loss requirement in the frequency band nearly from 2.84 to 8.2 GHz with a band-notch almost within 5.11–5.69 GHz band. This band-notch is corresponding to the WLAN and HIBERLAN/2 services. The proposed antenna is fabricated and the measured data of the return loss showed a good agreement with the simulated results. The proposed antenna featured suitable radiation patterns with good gain flatness over the UWB frequency band excluding the rejection band. The prototype antenna was integrated with three different band-notch techniques, almost similar performance was obtained. However, the three techniques were introduced for sake of completion and to provide flexibility of choice for different applications. It is noted that the proposed band-notched antenna is smaller in size (65%) and less complex compared to those of similar radiating element available in literature. Also the proposed antenna has a better performance regarding the gain and radiation efficiency over the operated frequency band. Such satisfactory performances and features make the proposed proximity-feed antenna a good candidate for UWB applications.

### REFERENCES

1. Agrawal, N. P., G. Kumar, and K. P. Ray, "Wide-band planar monopole antenna," *IEEE Trans. Antennas Propag.*, Vol. 46, No. 2, 294–295, Feb. 1998.
2. Jafari, H. M., M. J. Deen, S. Hranilovic, and N. K. Nikolova, "Slot antenna for ultra-wideband applications," *IEEE AP-S Int. Symp.*, 1107–1110, Albuquerque, Jul. 2006.

3. Danideh, A., R. Sadeghi Fakhr, and H. R. Hassani, "Wideband co-planar microstrip patch antenna," *Progress In Electromagnetics Research Letters*, Vol. 4, 81–89, 2008.
4. Schantz, H. G. and G. P. Wolynec, "Ultra-wideband antenna having frequency selectivity," U.S. Patent Publication, No. 2003/0090436 A1, 2003.
5. Choi, W., K. Chung, J. Jung, and J. Choi, "Compact ultra-wideband printed antenna with band-rejection characteristic," *Electron. Lett.*, Vol. 41, No. 18, 990–991, Sep. 2005.
6. Chawanonphithak, K., C. Phongcharoenpanich, S. Kosulvit, and M. Krairiksh, "5.8 GHz notched UWB bidirectional elliptical ring antenna excited by circular monopole with curved slot," *Asia-Pacific Microwave Conf.*, 653–656, Dec. 2007.
7. Kim, Y. and D. H. Kim, "CPW-fed planar ultra wideband antenna having a frequency band notch function," *Electron. Lett.*, Vol. 40, No. 7, 403–405, Apr. 2004.
8. Ma, T. G. and S. J. Wu, "Ultrawideband band-notched folded strip monopole antenna," *IEEE Trans. Antennas Propag.*, Vol. 55, No. 9, 2473–2479, Sep. 2007.
9. Nguyen, C. and C. Hsieh, "Millimeter wave printed circuit spurline filters," *IEEE MTT-S Int. Microwave Symp. Digest*, 98–100, Jun. 1983.
10. Nguyen, F. C. and K. Chang, "On the analysis and design of spurline bandstop filters," *IEEE Trans. Microw. Theory Tech.*, Vol. 33, No. 12, 1416–1421, Dec. 1985.
11. Tu, W. H. and K. Chang, "Compact microstrip bandstop filter using open stub and spurline," *IEEE Microw. Wireless Compon. Lett.*, Vol. 15, No. 4, 268–270, Apr. 2005.
12. Kim, J., C. S. Cho, and J. W. Lee, "5.2 GHz notched ultra-wideband antenna using slot-type SRR," *Electron. Lett.*, Vol. 42, No. 6, 315–316, Mar. 2006.
13. Chang, T.-N. and M.-C. Wu, "Band-notched design for UWB antennas," *IEEE Antennas and Wireless Propag. Lett.*, Vol. 7, 636–640, 2008.
14. Zhang, Y., W. Hong, C. Yu, Z.-Q. Kuai, Y.-D. Don, and J.-Y. Zhou, "Planar ultrawideband antennas with multiple notched bands based on etched slots on the patch and/or split ring resonators on the feed line," *IEEE Trans. Antennas Propag.*, Vol. 56, No. 9, 3063–3068, Sep. 2008.
15. Kim, D.-O., N.-I. Jo, D.-M. Choi, and C.-Y. Kim, "Design of the novel band notched UWB antenna with the spiral loop

- resonators,” *PIERS Online*, Vol. 6, No. 2, 173–176, 2010.
16. Choi, J., S. Hong, and U. Kim, “The design of an UWB antenna with notch characteristic,” *PIERS Online*, Vol. 3, No. 7, 987–990, 2007.
  17. Angelopoulos, E. S., A. Z. Anastopoulos, D. I. Kaklamani, A. A. Alexandridis, F. Lazarakis, and K. Dangakis, “Circular and elliptical CPW-fed slot and microstrip-fed antennas for ultrawideband applications,” *IEEE Antennas and Wireless Propag. Lett.*, Vol. 5, No. 1, 294–297, 2006.
  18. Saad, A. A. R., E. E. M. Khaled, and D. A. Salem, “Novel design of proximity-fed ultra-wide band annular slot antenna,” *PIERS Proceedings*, 1429–1433, Suzhou, China, Sep. 12–16, 2011.
  19. Baena, J. D., J. Bonache, F. Martin, R. Marques, F. Falcone, T. G. Lopetegui, M. A. Laso, J. Garcia, I. Gil, and M. Sorolla, “Equivalent circuit models for split ring resonators and complementary split ring resonators coupled to planar transmission lines,” *IEEE Trans. Microw. Theory Tech.*, Vol. 53, 1451–1461, Apr. 2005.
  20. Montero-de-Paz, J., E. Ugarte-Munoz, F. J. Herraiz-Martinez, V. Gonzalez-Posadas, L. E. Garcia-Munoz, and D. Segovia-Vargas, “Multifrequency self-diplexed single patch antenna loaded with split ring resonators,” *Progress In Electromagnetics Research*, Vol. 113, 47–66, 2011.
  21. Wu, H. W., M. H. Weng, Y. K. Su, R. Y. Yang, and C. Y. Hung, “Propagation characteristics of complementary split-ring resonator for wide bandgap enhancement in microstrip bandpass filter,” *Microwave and Optical Technology Letters*, Vol. 49, No. 2, 292–295, 2007.
  22. Lee, Y. J. and Y. Hao, “Characterization of microstrip patch antennas on metamaterial substrates loaded with complementary split-ring resonators,” *Microwave and Optical Technology Letters*, Vol. 50, No. 8, 2131–2135, 2008.